IOP PUBLISHING JOURNAL OF PHYSICS: CONDENSED MATTER

J. Phys.: Condens. Matter **19** (2007) 436209 (13pp) doi:10.1088/0953-8984/19/43/436209

Electronic damping of atomic dynamics in irradiation damage of metals

D R Mason, J le Page, C P Race, W M C Foulkes, M W Finnis and A P Sutton

Department of Physics, Imperial College London, London SW7 2AZ, UK

E-mail: daniel.mason@imperial.ac.uk

Received 9 May 2007, in final form 31 July 2007
Published 26 September 2007
Online at stacks.iop.org/JPhysCM/19/436209

Abstract

We investigate the transfer of energy from a harmonically oscillating atom in a metal to the electronic subsystem, using a direct simulation method based on time-dependent tight-binding (TDTB). We present our results in terms of a viscous damping coefficient β to enable direct comparison with previous MD and Langevin dynamics simulations, over an ionic energy range relevant for radiation damage. Analysis of our results using time-dependent perturbation theory shows that the rate of energy transfer to the electrons is independent of the frequency of the driven atom at high electronic temperatures, but at low temperature may vary by an order of magnitude. Our simulations show β also to be dependent on the electronic temperature, the position of the atom within the unit cell and even the direction of oscillation. We conclude that a TDTB simulation can give the electronic damping for an infinite metal over a limited simulation time window dependent on system size, and show how to monitor errors in dynamic simulations due to finite-size effects.

(Some figures in this article are in colour only in the electronic version)

1. Introduction

When a high energy neutron enters a metal, an initial collision phase produces localized regions containing self-interstitial atoms (SIAs) and vacancies. This is followed by a rapid period of recombination of these defects. This is known as a displacement cascade and lasts less than 100 ps for a cascade size of 50 nm [1, 2]. Over the past two decades molecular dynamics (MD) simulations of the ions have been used to model small cascades. Such simulations determine the extent of recombination and hence the final population of point defects. The final defect population, in turn, is the starting point for kinetic Monte Carlo studies of interstitial and vacancy hopping and recombination, dislocation dynamics and embrittlement [3], and is of great interest for the modelling of fission and fusion reactor materials.

The energy of ions involved in a cascade is rapidly partitioned to neighbouring ions by sequences of collisions. Energy is also transferred from the energetic ions to the cooler electrons, at a rate dependent on the electron–ion coupling [4]. This coupling increases the rate of cooling of the ions, and hence a large electronic damping inhibits defect recombination [5]. The rate of cooling due to the electrons is often characterized by the electronic stopping power, defined as the rate of change of ionic energy with position. Lindhard and Scharff [6] were the first to derive a model for stopping power at high ion velocity due to the Coulombic interaction between the ion and the electron gas. Electronic stopping power has also been computed using a perturbative approach [7] and more generally from a LCAO approach [8]. However with analytic models it is often difficult to go beyond simple examples and so find quantitatively correct behaviour for complex geometries or general Hamiltonians in a dynamic simulation.

Energy dissipation to the electrons has been included directly in MD simulations as a viscous damping force of the form $-\beta \mathbf{V}_I$, where $\mathbf{V}_I$ is the velocity of ion I and β a suitable damping coefficient. β is therefore simply related to the stopping power by $\frac{\mathrm{d}E}{\mathrm{d}x} = -\beta|\mathbf{V}|_I$. This approach was adopted first by Caro and Victoria [9], who choose a form for β dependent on the local electronic density. Energy is then returned from the electrons to the ions as white noise with a Langevin thermostat, whose magnitude is chosen to give the required equilibrium temperature according to the fluctuation-dissipation theorem. Rather than use a noise term Finnis *et al* [5] consider a velocity dependent β in an attempt to include equilibration between the ions and electrons. The most recent model in this family is due to Duffy *et al* [10]. They extend the Langevin dynamics of Caro and Victoria with a dissipative damping term acting on high energy ions which heats the electronic subsystem. The electronic temperature is evolved with a heat diffusion equation, the local value of which is used to determine the magnitude of the stochastic forces.

In this paper we compute the electronic damping using a tight-binding approximation. We use an orthogonal TB Hamiltonian rather than time-dependent density functional theory (TDDFT) as tens of thousands of atoms would be needed to simulate a realistic displacement cascade, and we wish to report effects that would be seen in such a direct simulation method. The large system size is needed not just to allow room for the collision sequence to take place, but also to circumvent finite-size effects on the electronic structure of the system. For the first time we test the notion of a single isotropic viscous damping coefficient β with direct simulation: we show it is a complicated function of the position and velocity of the ions within the supercell and the electronic temperature. β may also more generally be a tensor function and dependent on the history of the evolution of the ionic state via the current state of the electronic density matrix, but we have not investigated these aspects.

We seek to calculate β in such a manner that it is possible to identify features which are caused by limitations of the Hamiltonian or finite-size effects, and those which are genuine deviations from isotropic viscous damping. Any high energy incident ion will perturb the electronic subsystem with a continuous spectrum of frequencies; typical frequencies of a high energy ion passing through a metal will be of the order $\mathbf{V}_I/d$, where d is the distance of closest approach between ions. For an energy of 10 keV and $d = 0.5$ Å (a choice small compared to a typical interplanar spacing for transition metals) these frequencies are a few PHz—orders of magnitude above phonon frequencies. We show in section 3 that not all frequencies will be damped equally. To show this unambiguously our simulations will be of a single ion driven at frequencies ranging from below the natural frequency up to and beyond the PHz regime.

Our simplified model has the great advantage that we can compare the results to time-dependent perturbation theory (section 2.1). Comparing our results to first-order perturbation theory suggests that TDTB is indeed suitable for modelling the electronic damping of ionic

motion with ionic kinetic energies up to 10 keV. The limitations on the energy range will be made explicit in section 3.

2. Theory

We seek to relate the perturbation to the electronic subsystem caused by a high energy ion impact to the electronic transitions which occur. From these transitions we can determine the energy that is transferred to the electrons and hence the rate at which the ion is damped. To facilitate analysis we drive at a single frequency a single ion embedded in a supercell. By fixing the positions of all other atoms, we can focus exclusively on the transfer of energy to the electronic subsystem.

For this work we are using a simple s-band TB Hamiltonian parameterized for 'copper' atoms [11]. The TB Hamiltonian $\hat{H}(t)$ is the sum of a time-independent component $\hat{H}^{(0)}$ and a time-dependent contribution $\hat{H}^{(1)}(t)$. The time-independent contribution is the Hamiltonian of the perfect crystal with the vibrating atom removed, i.e. the site of the vibrating atom is vacant. $\hat{H}^{(1)}(t)$ describes the hopping integrals between the vibrating atom and its neighbours. It also describes the time-dependent electron–electron interactions, which we approximate as follows:

$$E_{\mathrm{ee}}(t) = \tfrac{1}{2}U \sum_{\alpha} \left(\rho_{\alpha}(t) - \rho^{(a)}\right)^2, \tag{2.1}$$

where $\rho^{(a)}$ is the number of electrons associated with a neutral atom, and is a parameter of the model [11]. The number of electrons associated with the atom at site α is denoted $\rho_{\alpha}(t)$.

U is another parameter of the model and we set it to be equal to 7 V. The hardness (ionization potential minus electron affinity) of a Cu atom is approximately 6.5 eV; our choice of U is consistent with this. Although U values of order 10 V are commonly used to describe the Cu^{2+} ions in the insulating parent compounds of high-temperature superconductors [12], the value of U for pure Cu is lower, both because the atoms are not ionized and because of the metallic screening of the on-site Coulomb interaction.

The choice of U affects the magnitude of the on-site ionic charges during the oscillation [13], but we note that these charges are only of order 0.1% of an electron and that the corresponding self-consistent energy is only 10^{-7} eV per atom. The fluctuation of charges is not, therefore, a significant mechanism for energy transfer between ionic and electronic subsystems in our simulations. We have confirmed this by varying U from 0 to 20 V, which only affects the heating rate by 5%.

The sum in equation (2.1) is taken over all atomic sites. Thus

$$\hat{H}^{(1)}(t) = \hat{h}(\mathbf{R}_I(t)) + \hat{V}_{\mathrm{ee}}(t), \tag{2.2}$$

where $\hat{h}(\mathbf{R}_I(t))$ contains the hopping integrals to the vibrating atom, and $\hat{V}_{\mathrm{ee}}(t) = \delta E_{\mathrm{ee}}(t)/\delta\hat{\rho}$. $\hat{V}_{\mathrm{ee}}(t)$ in the atomic basis is diagonal with matrix elements $U(\rho_{\alpha}(t) - \rho^{(a)})$.

The electronic contribution to the binding energy is thus

$$E_{\mathrm{el}}[\hat{\rho}] = \mathrm{Tr}(\hat{\rho} - \rho^{(a)}\hat{1})\hat{H} - \mathrm{Tr}\ \hat{\rho}\hat{V}_{\mathrm{ee}}(t) + E_{\mathrm{ee}}(t), \tag{2.3}$$

where $\hat{\rho} = \hat{\rho}(t)$, $\rho^{(a)}\hat{1}$ is a constant diagonal matrix in the atomic basis with all elements equal to $\rho^{(a)}$, and $\hat{H} = \hat{H}^{(0)} + \hat{H}^{(1)}(t)$. The subtraction of $\mathrm{Tr}\ \hat{\rho}\hat{V}_{\mathrm{ee}}(t)$ corrects for the presence of this term in the first term $\mathrm{Tr}(\hat{\rho} - \rho^{(a)}\hat{1})\hat{H}$, and the addition of $E_{\mathrm{ee}}(t)$ includes the electron–electron interaction energy.

The evolution of the electronic density operator $\hat{\rho}(t)$ is computed using

$$\dot{\hat{\rho}}(t) = \frac{1}{\mathrm{i}\hbar}[\hat{H}(t), \hat{\rho}(t)]. \tag{2.4}$$

This equation is integrated using the Runge–Kutta 4th-order algorithm.

If equation (2.3) were evaluated in the Born–Oppenheimer limit we would find $E_{\mathrm{el}}[\hat{\rho} = \hat{\rho}_{\mathrm{BO}}]$ returns to exactly the same value at the same point in each cycle of oscillation; there would be no cumulative change of E_{el} with time. Therefore, we may define the cumulative energy transferred to the electrons at time t to be

$$\begin{aligned}\Delta E(t) &= E_{\mathrm{el}}[\hat{\rho}(t)] - E_{\mathrm{el}}[\hat{\rho}_{\mathrm{BO}}(t)] \\ &= -\int_0^t \mathbf{f}_I(t') \cdot \mathbf{v}_I(t')\,\mathrm{d}t' + \int_0^t \mathbf{f}_I^{(\mathrm{BO})}(t') \cdot \mathbf{v}_I(t')\,\mathrm{d}t',\end{aligned} \tag{2.5}$$

where $\mathbf{f}_I(t)$ is the force on atom I due to the interactions of the vibrating atom through $\hat{H}^{(1)}(t)$ using the density matrix $\hat{\rho}(t)$; $\mathbf{f}_I^{(\mathrm{BO})}(t)$ is the equivalent force calculated with $\hat{\rho}^{(\mathrm{BO})}(t)$, and $\mathbf{v}_I(t)$ is the instantaneous velocity of the vibrating atom.

The force $-\mathbf{f}_I(t)$ is given by

$$\begin{aligned}-\mathbf{f}_I(t) &= \nabla_I E_{\mathrm{el}}[\hat{\rho}(t)] \\ &= \sum_{\alpha \neq I} (\rho_{\alpha I} + \rho_{I\alpha})[\nabla_I H_{\alpha I}^{(1)}]_{V_{\mathrm{ee}}} \qquad (2.6) \\ &= \sum_{\alpha \neq I} (\rho_{\alpha I} + \rho_{I\alpha}) \nabla_I h_{\alpha I}, \qquad (2.7)\end{aligned}$$

where $[\nabla_I H_{\alpha I}^{(1)}]_{V_{\mathrm{ee}}}$ is the gradient of a hopping integral between the vibrating atom and one of its interacting neighbours, evaluated with a *frozen* electron–electron potential $\hat{V}_{\mathrm{ee}}$. A full discussion of electronic forces is given by Todorov [14].

At any given instant the frictional force on the vibrating atom is

$$\mathbf{F}_I(t) = \mathbf{f}_I(t) - \mathbf{f}_I^{(\mathrm{BO})}(t), \tag{2.8}$$

where the second term on the right hand side averages to zero over a complete cycle.

At time $t = 0$ the density matrix $\hat{\rho}$ is initialized to $\hat{\rho}_{\mathrm{BO}}$, with the vibrating atom in its equilibrium position, so that the entire crystal is perfect. In the atomic basis the initial density matrix has elements

$$\rho_{\alpha\beta} = (\rho_{\mathrm{BO}})_{\alpha\beta} = \sum_n \langle\alpha|n\rangle f_T(\epsilon_n) \langle n|\beta\rangle, \tag{2.9}$$

where

$$\hat{H}|n\rangle = \epsilon_n |n\rangle, \tag{2.10}$$

and

$$\hat{H} = \hat{H}^{(0)} + \hat{H}^{(1)}(t = 0). \tag{2.11}$$

In equation (2.9) $f_T(\epsilon)$ is the Fermi–Dirac distribution for the electronic temperature T and where the chemical potential has been adjusted so that $\mathrm{Tr}\,\hat{\rho} = N\rho^{(a)}$, where N is the number of atoms in the supercell. The Hamiltonian in equation (2.10) is diagonalized with periodic boundary conditions applied to the supercell, and for a wavevector only at the centre of the Brillouin zone. Thus, the eigenvalue spectrum $\{\epsilon_n\}$ in equation (2.10) is discrete, and this turns out to be highly significant when we discuss the frequency dependence of the electronic damping.

Multiple k-point sampling for the same size simulation cell does not significantly improve the estimate of the rate of energy transfer into the electrons. The perturbative analysis to be discussed below shows that the main errors in the calculated energy transfer rate are caused by the sparseness of the density of transitions: the limited selection of final states into which an electron in any given initial state is able to scatter may not be representative of the density of final states in a real solid. If we were to carry out a multi-k-point simulation with accurate k-point sampling, we would in effect be studying an infinite periodic lattice of identical copies of our supercell. Since the Hamiltonian of this infinite system remains periodic, the supercell Bloch wavevector k remains a good quantum number and electrons in states of any given k are only able to scatter into states of the same k. Including more k points in the supercell Brillouin zone therefore fails to increase the number of final states into which any given initial state may be scattered, and does not significantly improve our estimate of the rate of energy transfer into the electrons. This is a limitation of the use of periodic boundary conditions to model a non-periodic solid in which the Bloch momentum k is not conserved. The only effective way to improve the calculation is to increase the size of the supercell.

The vibrating atom is forced to undergo harmonic oscillations with angular frequency Ω and a constant amplitude $|\mathbf{A}| = 0.1$ Å:

$$\mathbf{R}_I(t) = \mathbf{R}_0 + \mathbf{A}\sin\Omega t. \tag{2.12}$$

The amplitude of the vibrating atom $|\mathbf{A}|$ is chosen large enough to create a significant perturbation in the electronic subsystem, but small enough that the electronic forces remain a linear function of the displacement to facilitate analysis with linear response theory.

The power injection into the electron gas is $\Delta E(\tau)/\tau = 2\beta_\Omega\langle K_I\rangle/m_I$, where we have assumed the frictional force may be expressed as $\mathbf{F}_I = -\beta_\Omega\mathbf{v}_I$, where β_Ω is a scalar which varies little over one oscillation. $\langle K_I\rangle$ is the average kinetic energy of atom I, and τ is the period of oscillation. It follows that

$$\beta_\Omega = \frac{2\Delta E(\tau)}{|\mathbf{A}|^2\Omega^2\tau}. \tag{2.13}$$

We have thus associated the energy change in our numerical simulations with the equivalent energy change that would be present in an MD simulation with a frictional force of the form $\mathbf{F}_I = -\beta_\Omega\mathbf{v}_I$.

2.1. Time-dependent perturbation theory

Choosing the form of the perturbation on the system to be a displacement of a single ion at a single frequency simplifies the analysis of our results. In the long-time limit for a continuum system, we can find a simple integral expression for the electronic damping β_Ω in equation (2.13) using Fermi's golden rule (FGR).

We have found that our numerical simulation results change little if we do not include the electron–electron interactions (equation (2.1)). The model is well approximated by splitting the electronic Hamiltonian into equilibrium and a periodic perturbation part neglecting electron–electron interactions; $\hat{H}(t) \cong (\hat{H}^{(0)} + \hat{h}(t = 0)) + (\hat{h}(t) - \hat{h}(t = 0))$. As we use small displacements, we can write the perturbation in terms of a force operator $\hat{F}$,

$$\hat{h}(t) - \hat{h}(t = 0) \cong (\nabla_I\hat{h}(t = 0)) \cdot (\mathbf{R}_I(t) - \mathbf{R}_0) = -\hat{F}A\sin(\Omega t). \tag{2.14}$$

First-order perturbation theory gives the energy change of the electronic subsystem as an integral over the band of the system-dependent and time-dependent terms:

$$\Delta E(t) = \int_{-\infty}^{\infty} q_T(\varepsilon)s(\varepsilon, \Omega; t)\,\varepsilon\,\mathrm{d}\varepsilon. \tag{2.15}$$

$q_T(\varepsilon)$ gives the rate at which electronic transitions with energy change ε can occur in a system initially with a temperature T,

$$q_T(\varepsilon) = \left(\frac{A}{2\hbar}\right)^2 \sum_{\mathbf{k}} \sum_{\mathbf{k}' \neq \mathbf{k}} |F_{\mathbf{k}'\mathbf{k}}|^2 \, f_T(\epsilon_{\mathbf{k}'})(1 - f_T(\epsilon_{\mathbf{k}'} + \varepsilon))\delta(\varepsilon - \epsilon_{\mathbf{k}} + \epsilon_{\mathbf{k}'}). \tag{2.16}$$

$|\mathbf{k}\rangle$ denotes the eigenstates of the equilibrium Hamiltonian. $F_{\mathbf{k}'\mathbf{k}}$ is the matrix element $\langle \mathbf{k}', \hat{F}\mathbf{k}\rangle$. $q_T(\varepsilon)$ thus contains all the system-dependent information about the rate at which the electrons may absorb energy.

As the system size increases, the discrete energy levels $\{\epsilon_j\}$ become ever more closely spaced, and equation (2.16) tends to the integral

$$\begin{aligned} &\lim_{N\to\infty} q_T(\varepsilon) = \left(\frac{A}{2\hbar}\right)^2 \int_{\text{band}} f_T(e)(1 - f_T(e + \varepsilon))|\tilde{F}_{e,e+\varepsilon}|^2 \, \mathrm{d}e, \\ &\text{where } |\tilde{F}_{e,e+\varepsilon}|^2 = \frac{V}{8\pi^3} \int_{S(e)} \mathrm{d}^2\mathbf{k} \frac{V}{8\pi^3} \int_{S(e+\varepsilon)} \mathrm{d}^2\mathbf{k}' \frac{|\langle \mathbf{k}', \hat{F}\mathbf{k}\rangle|^2}{|\mathbf{v}_{\mathrm{g}}(\mathbf{k})||\mathbf{v}_{\mathrm{g}}(\mathbf{k}')|}. \end{aligned} \tag{2.17}$$

$S(e)$ is the isoenergetic surface consisting of all eigenstates with energy e. $\mathbf{v}_{\mathrm{g}}$ is the group velocity. V is the volume of the simulation cell.

The second term in the integrand in equation (2.15), $s(\varepsilon, \Omega; t)$, samples $q_T(\varepsilon)$ at time t given that the driving force is at frequency Ω,

$$\begin{aligned} s(\varepsilon, \Omega; t) = {} & t^2 \mathrm{sinc}^2\left(\left[\frac{\varepsilon + \hbar\Omega}{2\hbar}\right] t\right) + t^2 \mathrm{sinc}^2\left(\left[\frac{\varepsilon - \hbar\Omega}{2\hbar}\right] t\right) \\ & - 2t^2 \cos(\Omega t) \, \mathrm{sinc}\left(\left[\frac{\varepsilon + \hbar\Omega}{2\hbar}\right] t\right) \mathrm{sinc}\left(\left[\frac{\varepsilon - \hbar\Omega}{2\hbar}\right] t\right). \end{aligned} \tag{2.18}$$

The sinc squared functions in equation (2.18) narrow, such that their widths reduce as $1/t$ and the total area under them, $t^2\mathrm{sinc}([\frac{\varepsilon \pm \hbar\Omega}{2\hbar}]t)$, increases linearly with time. Therefore for long times we obtain

$$\lim_{\text{large } t} s(\varepsilon, \Omega; t) = 2\hbar\pi t \, (\delta(\varepsilon + \hbar\Omega) - \delta(\varepsilon - \hbar\Omega)). \tag{2.19}$$

We therefore arrive at the familiar FGR result for large system sizes and long times, which can be written in the form

$$\Delta E(t) = \frac{A^2 \pi \Omega t}{2} \int_{-\infty}^{\infty} \left(f_T(\varepsilon - \frac{1}{2}\hbar\Omega) - f_T(\varepsilon + \frac{1}{2}\hbar\Omega)\right) |\tilde{F}_{\varepsilon - \frac{1}{2}\hbar\Omega, \varepsilon + \frac{1}{2}\hbar\Omega}|^2 \, \mathrm{d}\varepsilon. \tag{2.20}$$

The electronic damping (equation (2.13)) measured in our simulations, provided the assumptions described above are met, should then be

$$\beta_{\Omega,\mathrm{FGR}} = \frac{\pi}{\Omega} \int_{-\infty}^{\infty} \left(f_T(\varepsilon - \frac{1}{2}\hbar\Omega) - f_T(\varepsilon + \frac{1}{2}\hbar\Omega)\right) |\tilde{F}_{\varepsilon - \frac{1}{2}\hbar\Omega, \varepsilon + \frac{1}{2}\hbar\Omega}|^2 \mathrm{d}\varepsilon. \tag{2.21}$$

$\beta_{\Omega,\mathrm{FGR}}$ will be frequency independent if the integral is proportional to Ω. It will have an electronic temperature-dependence given by the difference in Fermi factors $f_T(\varepsilon - \frac{1}{2}\hbar\Omega) - f_T(\varepsilon + \frac{1}{2}\hbar\Omega)$, and it will be dependent on the Hamiltonian through $\tilde{F}_{\varepsilon - \frac{1}{2}\hbar\Omega, \varepsilon + \frac{1}{2}\hbar\Omega}$. We will explore the limits of equation (2.21) in section 3. In section 4 we explore when the FGR assumptions are *not* met when simulating a finite-size system for a finite-time interval.

3. Results

In this section we analyse the dependence of the damping β_Ω on electronic temperature, driving frequency, the direction of oscillation and the position of the oscillating ion in the unit cell. When running simulations we were careful to use large enough system sizes to ensure that the results obtained corresponded to those of an infinitely large metal (see section 4).

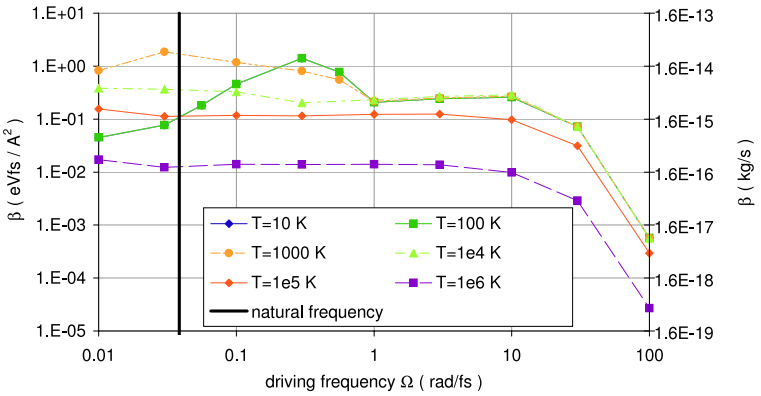

Figure 1. The damping coefficient β computed from simulations at a range of driving frequencies and electronic temperatures. The $T = 10$ and 100 K lines coincide. At high temperatures ($T > 10^5$ K) the damping is independent of frequency Ω until $\hbar\Omega$ is comparable with the bandwidth. At low temperatures and low frequencies we see variation in β_Ω due to the inhomogeneity of the electronic structure. The lines are to guide the eye.

3.1. Damping as a function of driving frequency and temperature

We now explore the dependence of the rate of change of the electronic energy on the frequency of the ion oscillation and the initial state of the electronic system. We drive the atom about the equilibrium point $\mathbf{R}_0 = [000]$, i.e. an ideal lattice site, at a range of frequencies and with the density matrix initialized at different electronic temperatures. The computational repeat cell comprises $8 \times 7 \times 5$ fcc unit cells, and the oscillator is driven in the long [100] direction. Figure 1 shows our results.

We analyse the main features of this graph using the analysis presented in section 2.1 to highlight when the form of the electron–ion coupling is important. The analysis will focus on the form of the function $|\tilde{F}_{\varepsilon-\frac{1}{2}\hbar\Omega,\varepsilon+\frac{1}{2}\hbar\Omega}|^2$, which is the only term of (2.21) through which the choice of tight-binding model enters. A contour plot of $|\tilde{F}_{\varepsilon-\frac{1}{2}\hbar\Omega,\varepsilon+\frac{1}{2}\hbar\Omega}|^2$ is shown in figure 2.

(i) In figure 1 we see a marked decrease of the damping at the highest frequencies, $\Omega > 10$ rad fs^{-1}. For such high energies the number of available electronic transitions with such an energy difference begins to drop significantly. This is seen in the low magnitude of the high Ω values of the contour plot in figure 2(a). We are therefore unable to transfer energy efficiently to the electrons in this regime. This is a failure of the simple s-band tight-binding model we are using—a real metal would allow transitions to higher bands. However, these frequencies are beyond those which would be generated by a 10 keV ion.

(ii) For electronic temperatures below 10 000 K and frequencies over the range 0.01–1 rad fs^{-1} we see a variation of over an order of magnitude in the damping with frequency. For the temperatures considered here the Fermi functions term of (2.21) has the approximate form of a 'top hat' of width $\hbar\Omega$ centred on the Fermi energy. Figure 2(b) shows how $|\tilde{F}_{\varepsilon-\frac{1}{2}\hbar\Omega,\varepsilon+\frac{1}{2}\hbar\Omega}|^2$ varies with ε for a number of different Ω. The dependence of β_Ω on Ω therefore arises from the difference between the area under the different curves over the intervals $(\varepsilon_F - \frac{1}{2}\hbar\Omega, \varepsilon_F + \frac{1}{2}\hbar\Omega)$. The similarity of the curves over a large interval about the Fermi level suggests that the main contribution to the variation of β_Ω with Ω is from the width of the Fermi function top hat. The variation in the number of transitions between isoenergetic surfaces separated by $\hbar\Omega$, the main contribution to $\tilde{F}$, is less influential for this frequency range.

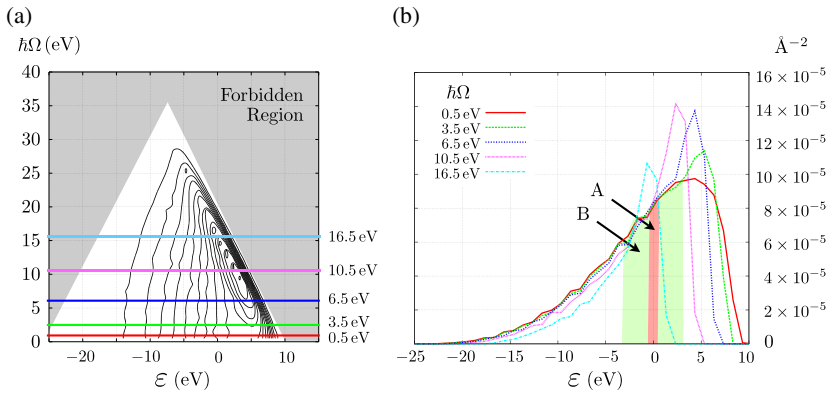

Figure 2. Plots of $|\tilde{F}_{\varepsilon-\frac{1}{2}\hbar\Omega,\varepsilon+\frac{1}{2}\hbar\Omega}|^2$ (equation (2.17)), which determines how the damping is influenced by the choice of tight-binding model. The ε axis has been shifted so $\varepsilon = 0$ corresponds to the Fermi energy. (a) A contour plot of $|\tilde{F}|^2$. The contours are linearly distributed. (b) Slices of the contour plot at given frequencies. At low temperatures the damping at Ω can be found by determining the area under the curve in an interval of width $\hbar\Omega$ about the Fermi energy (see section 3.1). This area is shown as a shaded region for A: $\hbar\Omega = 0.5$ eV and B: 3.5 eV. The plots were created by using time-independent perturbation theory to determine an analytic formula for $E(k)$ and then collecting this data in 1 eV bins for a system of $25 \times 22 \times 20$ unit cells.

(iii) At high electronic temperatures, $T > 10^4$ K, we see very little variation with frequency until the high energy cut-off described in (i). At high temperature the Fermi function term of (2.21) simplifies to

$$f_T\left(E - \frac{1}{2}\hbar\Omega\right) - f_T\left(E + \frac{1}{2}\hbar\Omega\right) \approx \frac{\hbar\Omega}{4k_B T} \tag{3.1}$$

where k_B is Boltzmann's constant. Since this term is energy independent we find that the electronic damping is given by

$$\beta_{\Omega,\mathrm{FGR}} = \frac{\hbar\pi}{4k_B T}\int_{\mathrm{band}} |\tilde{F}_{\varepsilon-\frac{1}{2}\hbar\Omega,\varepsilon+\frac{1}{2}\hbar\Omega}|^2 \,\mathrm{d}\varepsilon. \tag{3.2}$$

Here the Fermi function term that was so influential in the low temperature case no longer has an energy dependence. In the high temperature case we integrate over the whole band for every Ω. All the electrons can make transitions regardless of the frequency of perturbation. The damping therefore depends only on how the total number of transitions with a given energy change varies with this energy difference. From figure 2 this variation is small until the frequencies referred to in (i). Therefore the variation of β_Ω with Ω is small relative to that of the low-temperature regime. We can also see from equation (3.2) that β_Ω scales with inverse temperature.

3.2. Damping as function of direction and position

Next we consider driving the atom in different directions, and about different positions $\mathbf{R}_0$. Our intention is not to produce a full survey of β as a function of driving direction and atomic position, only to note the degree to which variation from a single scalar might occur. We restrict our interest to high symmetry points, plus interpolating midpoints. We use a cube of $7 \times 7 \times 7$ fcc unit cells, driven with fixed oscillator frequency $\Omega = 1$ rad fs^{-1} and initial electronic temperature $T = 1000$ K. Results are shown in figure 3.

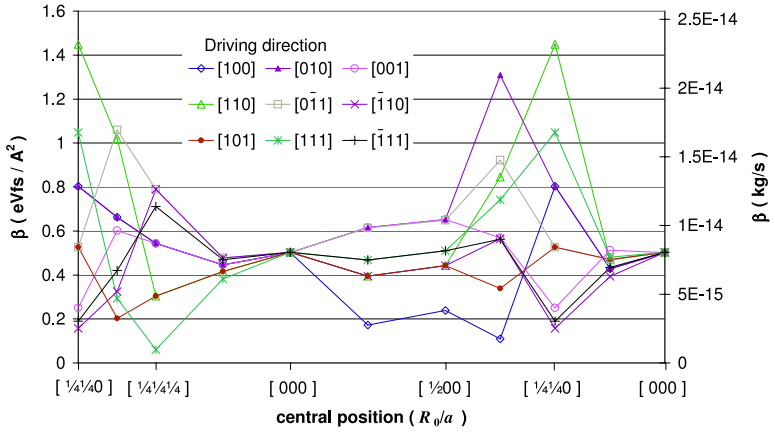

Figure 3. The damping coefficient β computed for different driving directions for the oscillator starting from different fractional positions within the fcc unit cell, as indicated along the horizontal axis. β is isotropic only for small amplitude oscillations about the ideal lattice site. More generally it is dependent on direction and the position of the atom in the unit cell. The lines are to guide the eye.

The variation in the damping is seen to be less than one order of magnitude. However β is isotropic only when the atom is driven about its ideal lattice site: this isotropy is expected given the cubic symmetry at this point[1].

Taken with the results of section 3.1, these results demonstrate the structure that arises in the damping when we consider an explicit representation of the electron system. Furthermore the frequency and electronic temperature ranges relevant for radiation damage are those with the most substantial dependence on electronic structure. We have also found that it is the behaviour at positions away from the lattice points, something obviously important for MD simulations, which has the most significant directional dependence.

4. Finite size effects

In section 2.1 we derived a form for $\beta_{\Omega,\mathrm{FGR}}$ at long times (equation (2.21)), assuming that the spectrum of available transitions $q_T(\varepsilon)$ was continuous. For any finite-sized system $q_T(\varepsilon)$ will be a discrete sum, as in equation (2.16), and so the long-time limit must be approached with more care. The maximum time over which any damping can be sensibly measured will be when the width of the sinc squared functions in equation (2.18) become sufficiently small that the discreteness of $q_T(\varepsilon)$ is noticeable.

We can get a rough order-estimate for the number of transitions which are sampled at time t as follows: if $\hbar\Omega > 2k_\mathrm{B}T$ a phonon of energy $\hbar\Omega$ may not be emitted by an electronic transition. The precision of the power transfer calculation will be limited by the density of available phonon absorbing transitions. Only states within the range $\max(0, \min(2k_\mathrm{B}T + \hbar\Omega, E_\mathrm{b} - \hbar\Omega))$ can be stimulated, where E_b is the electronic bandwidth. As the width of $\mathrm{sinc}^2(\varepsilon t/\hbar)$ is $\Delta\varepsilon = 4\pi\hbar/t$, this gives a number of transitions at time t:

$$n \approx \left(\frac{N}{E_\mathrm{b}}\right)^2 \max(0, \min(2k_\mathrm{B}T + \hbar\Omega, E_\mathrm{b} - \hbar\Omega))\frac{4\pi\hbar}{t}, \tag{4.1}$$

[1] At point $[\frac{3}{8}\frac{1}{8}0]$ the β values for three different driving directions almost coincide. This we believe to be no more than chance—there is no reason for this due to the crystal symmetry.

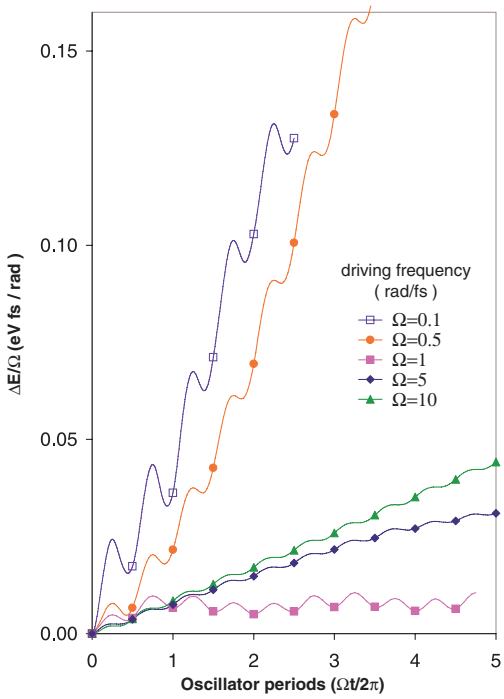

Figure 4. The energy transfer (defined in equation (2.5)) to the electronic subsystem as a function of time. The supercell used was $8 \times 7 \times 5$ unit cells, and the ion driven in the [100] direction about the lattice point. Symbols on the curves indicate where the oscillator passes through the point $\mathbf{R}_I = \mathbf{R}_0$. If β were perfectly independent of driving frequency these marks would coincide and would fall on a line of constant gradient. We see that the $\Omega = 1$ and $\Omega = 5$ lines diverge from linear behaviour at later times. $\Omega = 0.1$ and $\Omega = 0.5$ do not achieve linearity until after the first period.

where we have assumed that the N electronic eigenstates are distributed evenly over the bandwidth. If $\hbar\Omega < 2k_\mathrm{B}T$ precision is limited by the smaller range of available phonon emitting transitions. Then

$$n \approx \left(\frac{N}{E_\mathrm{b}}\right)^2 (\min(2k_\mathrm{B}T, E_\mathrm{b}) - \hbar\Omega)\frac{4\pi\hbar}{t}. \tag{4.2}$$

A maximum time for a dynamic simulation would then be given by ensuring n is greater than some small integer.

Equation (2.18) also gives a minimum time where we might expect the FGR behaviour to apply: at small t not only must the high moments of q_T be small in the sampled region, but also the cross term in equation (2.18) must be negligible. The latter condition occurs when the separation between the sinc functions ($2\hbar\Omega$) is large compared to their width, giving $t_\mathrm{min} > \pi/\Omega$. The damping experienced immediately after an impulse may be quite different from the steady-state response.

The system sizes we have used here are adequate to provide a (sometimes short) window where the continuum long-time damping response can be computed numerically. Repeating the numerical simulations of section 3 with a larger supercell shows that our results for β have converged to within 5% of their infinite size limits. The value of β given by the simulation also agrees with analytic results prepared from linear response theory (equation (2.21)). Figure 4 shows a plot of the energy change as a function of time for different driving frequencies.

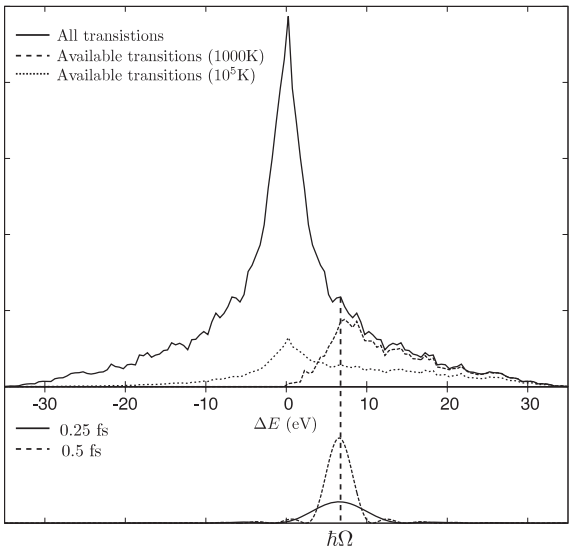

Figure 5. Analytic results suggest (equation (2.21)) that we can determine the electronic damping by considering the function $q_T(\varepsilon)$ (upper plot) weighted by a sinc function (lower plot). Upper: from the full density of transitions (dark line) $q_T(\varepsilon)$ (equation (2.16)) at 1000 K and 10^5 K is obtained by imposing Fermi–Dirac occupancies and the electron–ion coupling term. Lower: $s(E, \Omega; t)$ (equation (2.18)). As time evolves the sinc^2 function will narrow and the discrete nature of the density will become increasingly important. In this illustration $|\tilde{F}_{\varepsilon-\frac{1}{2}\hbar\Omega,\varepsilon+\frac{1}{2}\hbar\Omega}|^2$ has been set to 1 to simplify evaluation. The histogram is computed for $15 \times 12 \times 10$ unit cells with 0.5 eV bins.

At $\Omega < 1$ rad fs^{-1} the minimum time is evident, with a one-period lead in before linear behaviour sets in. The $\Omega > 1$ rad fs^{-1} lines show linearity breaking down after a time limit. $\Omega = 1$ rad fs^{-1} is chosen as it happens to be an anomalous point where the available transitions are abnormally sparse for this supercell. Note that the energy transfer is not a monotonic function of time over each oscillation: $\mathbf{F}_I$ can not be simply written as a constant multiple of $\mathbf{V}_I$. Using a time-independent β is only valid as an average over a number of cycles.

In a full dynamic simulation involving many moving ions it will be very difficult to ensure that the available transitions are sampled correctly to avoid finite-size effects. For any finite-sized simulation there will be some frequencies which are incorrectly damped owing to a lack of available electronic transitions. Our methodology exaggerates this problem by driving at a single frequency; we believe that such problems are unlikely to be severe for system sizes $N > 1000$ in dynamic simulations. Firstly all driving frequencies would be present in such a simulation, and secondly as the atoms move degeneracies in the electronic states would be lifted, smoothing the density of states. If desired we could monitor the situation by checking for undesirable structure in a histogram of $q_T(\varepsilon)$. Such a histogram is illustrated in figure 5.

5. Conclusion

We have used time-dependent tight-binding simulations to investigate the energy transfer from an ion executing harmonic motion. The frequencies were chosen to be relevant to the simulation of radiation damage in metals. In order to compare our results with techniques used in MD we defined a damping from the energy change given by our simulations.

It is difficult to extract from the literature a single value for the damping coefficient for a copper ion moving in copper. Ziegler *et al* [15] offer $\beta = 1.913 \times 10^{-13}$ kg s^{-1} = 11.96 eV fs Å^{-2}, which is the value used by the TRIM code. Finnis *et al* [5] suggest a limiting case $\beta = 2.49 \times 10^{-14}$ kg s^{-1} = 1.55 eV fs Å^{-2}. Wang *et al* [16] calculate $\beta = 3.81 \times 10^{-15}$ kg s^{-1} = 0.238 eV fs Å^{-2}. These results span two orders of magnitude. Our result (β between 10^{-15} and 10^{-14} kg s^{-1}) is within this range, but should not be compared uncritically. Our computed value is very sensitive to the density of states at the Fermi level, which is not fitted well by the simple TB model. It is also the damping of a single moving ion rather than a grossly damaged collision region.

Our results show that at high electronic temperatures the damping due to the electronic system is frequency independent. However for temperatures below 10^4 K and angular frequencies up to 10 rad fs^{-1} the damping varies depending on the frequency of oscillation. This parameter regime is that which is encountered in irradiation damage experiments. Our results also indicate that when considering oscillations about interstitial points directional dependence is important. The behaviour of particles at interstitial points is an important factor in displacement cascades. This preliminary work therefore indicates that a complex tensor damping may be required for an accurate representation of electronic effects in MD. Nevertheless our results offer support that the inclusion of a scalar damping can give the effect of electrons to within an order of magnitude.

This additional complexity is naturally included in simulations which use the TDTB formalism throughout. Analysis from perturbation theory shows that this additional structure to β stems directly from considering an electronic system with structure. We have seen our tight-binding model fail when the driving frequency is high and the electrons are no longer able to absorb energy because there are no available transitions between electronic states. A more subtle problem occurs when the discreteness in the spectrum of available transitions becomes important in determining the electron energy change. While this effect can be mostly alleviated by increasing the system size, specific frequencies may still be affected by this kind of error. This problem is highlighted by using a single driving frequency—in a real dynamic simulation many frequencies are present so the impact of a single frequency is lessened.

Acknowledgments

The authors would like to thank Andrew Horsfield and Tchavdar Todorov for helpful discussions. DRM and CPR were supported by EPSRC grant number EP/C524403 and JleP by the States of Guernsey. APS gratefully acknowledges the support of a Royal Society Wolfson Merit Award.

References

[1] Schilling W 1978 *Hyperfine Interact.* **4** 636–44
[2] Phythian W J, Stoller R E, Foreman A J E, Calder A F and Bacon D J 1995 *J. Nucl. Mater.* **223** 245–61
[3] Wirth B D, Odette G R, Marian J, Ventelon L, Young-Vandersall J A and Zepeda-Ruiz L A 2004 *J. Nucl. Mater.* **329** 103–11
[4] Flynn C P and Averback R S 1988 *Phys. Rev.* B **38** 7118–7120
[5] Finnis M W, Agnew P and Foreman A J E 1991 *Phys. Rev.* B **44** 567–74
[6] Lindhard J and Scharff M 1961 *Phys. Rev.* **124** 128–30
[7] Falcone G and Sroubek Z 1989 *Phys. Rev.* B **39** 1999–2003
[8] Dorado J J and Flores F 1993 *Phys. Rev.* A **47** 3062–72
[9] Caro A and Victoria M 1989 *Phys. Rev.* A **40** 2287–91

[10] Duffy D M and Rutherford A M 2007 *J. Phys.: Condens. Matter* **19** 1–11
[11] Sutton A P, Todorov T N, Cawkwell M J and Hoekstra J 2001 *Phil. Mag.* A **81** 1833–48
[12] Hybertsen M S, Schluter M and Christensen N E 1989 *Phys. Rev.* B **39** 9028–41
[13] Goringe C M, Bowler D R and Hernández E 1997 Tight-binding modelling of materials *Rep. Prog. Phys.* **60** 1447–512
[14] Todorov T N 2001 *J. Phys.: Condens. Matter* **13** 10125–48
[15] Ziegler J F, Biersack J P and Littmark U 1985 *The Stopping and Range of Ions in Solids* (Oxford: Pergamon)
[16] Wang Z G, Dufour C, Paumier E and Toulemonde M 1994 *J. Phys.: Condens. Matter* **6** 6733–50